Structure and piezoelectric properties of Sm-doped $BiFeO_3$ ceramics near the morphotropic phase boundary

D.V. Karpinsky [1, 2*], I.O. Troyanchuk [1], A.V. Trukhanov [1], M. Willinger [3], V.A. Khomchenko [4], A.L. Kholkin [5], V. Sikolenko [6], T. Maniecki [7], W. Maniukiewicz [7], S.V. Dubkov [2], M.V. Silibin [2]

[1] Scientific-Practical Materials Research Centre of NAS of Belarus, 220072 Minsk, Belarus
[2] National Research University of Electronic Technology "MIET", 124498 Zelenograd, Moscow, Russia
[3] Fritz-Haber-Institut der Max-Planck-Gesellschaft, D-14195 Berlin, Germany
[4] CFisUC, Department of Physics, University of Coimbra, P-3004-516 Coimbra, Portugal
[5] Department of Physics, University of Aveiro, 3810-193 Aveiro, Portugal
[6] Joint Institute for Nuclear Research, 141980 Dubna, Russia
[7] Institute of General and Ecological Chemistry, Lodz University of Technology, 90-924 Lodz, Poland

Abstract

The evolution of crystal structure and piezoelectric properties of the $Bi_{1-x}Sm_xFeO_3$ ceramics with compositions corresponding to the phase boundary region between the polar rhombohedral and anti-polar orthorhombic phases have been studied. The materials have been investigated using X-ray diffraction, transmission electron microscopy and piezoresponse force microscopy techniques. The diffraction measurements have allowed studying the crystal structure transformations depending on the dopant concentration and temperature. Similar to the compounds with $x > 0.18$, the lightly-doped samples have been found to adopt the non-polar orthorhombic structure at elevated temperatures. The research has clarified the correlation between the structural state and piezoelectric behavior. Substantial increase in piezoresponse observed for the phase-separated compounds having a dominant fraction of the rhombohedral phase has been discussed assuming significant extrinsic contribution associated with a metastable structural state changing under external electric field.

Keywords: *multiferroics; X-ray diffraction; piezoresponse; electron microscopy; phase transition*

Introduction

Complex transition metal oxides attract scientific interest during the last decades due to the multiple phase transitions and related changes in the physical properties [1-7]. The most pronounced enhancement of the physical parameters has been observed for the $BiFeO_3$-based compounds within the morphotropic phase boundaries [8-10] where their crystal structure is notably sensitive to external stimuli such as temperature, electric and magnetic field, mechanical stress, radiation etc. The results of structural studies performed for these compounds assume that the related structural state is associated with a coexistence of the adjacent phases with a typical size reduced down to nanometer level or denotes a formation of novel intermediate phases with crystal symmetry lower than those attributed to the adjacent microscopic phases [11-15].

One of the methods to form metastable structural state in the $BiFeO_3$-based compounds is a chemical doping at A- and/or B- positions of perovskite lattice of the parent $BiFeO_3$. It is known that chemical substitution of bismuth ions by rare-earth

author to whom correspondence should be addressed: karpinski@ua.pt

elements with relatively large ionic radii (La - Sm) drives structural transition from the rhombohedral (R) phase to the anti-polar orthorhombic (O_2) phase and then to the non-polar orthorhombic (O_1) phase via the two-phase regions [16-21]. The compounds at the phase boundary R - O_2 are of particular interest since their specific structural state is associated with enhanced physical properties promising for device applications.

$BiFeO_3$-based compounds doped with lanthanum and praseodymium ions are characterized by the widest compositional range of the coexistent rhombohedral and anti-polar orthorhombic phases ($\Delta x \sim 0.05$), possess the broadest concentration ranges for the single phase rhombohedral and orthorhombic state, and have the most pronounced physical properties among the rare-earth-doped solid solutions [19, 22-25]. Chemical doping with rare-earth ions having the smaller ionic radii leads to a shortening of the compositional ranges attributed to the phase coexistence and single phase states. Moreover, the compounds doped with the ions having the radii smaller than that of Sm^{3+} exhibit the concentration-driven transition directly to the non-polar orthorhombic phase without the formation of the anti-polar orthorhombic phase [26].

Samarium doped compounds attract particular attention due to the narrow concentration range attributed to the phase coexistence state and single phase orthorhombic state at room temperature [15, 27, 28]. Nanoscale clusters of the adjacent anti-polar orthorhombic phase unavoidably presented in the dominant rhombohedral phase near the related phase boundary act as defects which modify physical properties of the compounds and result in a reduction of structural stability of the compounds. Reduced stability of this structural state under external stimuli such as electric and magnetic field paves the way for the developing and production of the new effective functional materials with tunable physical parameters. In particular, $BiFeO_3$-based compounds with compositions near the MPB demonstrate significant change in electrical resistance, polarization and remnant magnetization under an external electric or magnetic field, which makes these materials promising for production of memristors [29], magnetoelectric sensors [30, 31], elements of non-volatile memory and spin field-effect transistors [32]. There are several concepts used to justify enhanced piezoelectric response observed for these materials near the MPB. Field-induced transition from the anti(non)-polar orthorhombic phase into the polar active rhombohedral phase has been considered by D. Kan and co-workers [16] as the origin of the enhanced piezoelectric response. Another concept considers significant contribution of extrinsic component of the piezoresponse due to domain wall-related effects [33, 34]. The next mechanism used to explain the enhancement of the properties is associated with easy paths for polarization rotation observed for the compounds at the morphotropic boundary separating two phases with different orientations of polarization [8, 35]. Proximity of the unit cell parameters attributed to the different structural phases in the vicinity of the phase boundary regions hampers determination of the crystal structure of the related compounds which impedes the understanding of the correlation between the structural state and physical properties. The present study is focused on the temperature evolution of the crystal structure of samarium doped compounds having the two-phase structural state at room temperature. The obtained results have allowed to determine temperature stability ranges of the structural phases at the phase boundary region as well as to clarify the relationship between the structural state and electromechanical properties of the $BiFeO_3$-based

multiferroics. The electric filed-induced structural transition observed in the $Bi_{1-x}Sm_xFeO_3$ samples at the rhombohedral-orthorhombic phase boundary is considered.

Experimental

The $Bi_{1-x}Sm_xFeO_3$ ($0 \le x \le 0.25$) ceramic samples were prepared via a two-stage solid phase synthesis. The initial high purity oxides (Bi_2O_3, Sm_2O_3, Fe_2O_3, Alfa Aesar, purity >99.9%) were taken in the stoichiometric ratio and thoroughly mixed for 30 min in a planetary mill RETSCH PM-100 using high purity isopropyl alcohol as a medium. The samples have been firstly annealed at 800 °C for 3h and then processed at the final synthesis temperature (870°C for x=0, 930 °C for x=0.1, 935 °C for x=0.11, 940 °C for x=0.12, 945 °C for x=0.13, 950 °C for x=0.14, 955 °C for x=0.15, 1030 °C for x=0.2 and 1060 °C for x=0.25) for about 12 h. After the synthesis the samples were quenched down to room temperature. X-ray diffraction measurements were made on a Rigaku D/MAX-B diffractometer with Cu *K*α radiation. The XRD data were analyzed by the Rietveld method using the FullProf software [36]. Electromechanical properties of the compounds were investigated with piezoresponse force microscopy (PFM) using a NTEGRA Prima (NT-MDT) commercial setup by applying *ac* voltage with an amplitude of 5 V and a frequency of 100 kHz. The PFM loops were measured in pulse mode [37]. High-resolution transmission electron microscopy (HRTEM) measurements have been performed using a FEI aberration-corrected Titan 80–300 microscope operating at 300 kV and equipped with an EDX detector.

Results and discussion

Evolution of the crystal structure as a function of the dopant content and temperature.

The X-ray diffraction measurements performed for the solid solutions $Bi_{1-x}Sm_xFeO_3$ have testified single-phase state with rhombohedral crystal structure (space group *R3c*) for the compounds with $x \le 0.1$, the obtained data being in accordance with the previously published results [38, 39]. The unit cell parameters gradually decrease with increasing the dopant concentration; angle $alfa_R$ which specifies rhombohedral distortion increases with Sm content and thus denotes a reduction of the structural distortion. At the same time, there is a decrease in the off-center displacements of the Bi(Sm) and Fe ions which determine polar character of the rhombohedral structure. Refinement of the room temperature diffraction patterns obtained for the compounds within the concentration range $0.1 < x < 0.15$ has allowed to determine the phase ratio at the phase coexistence region. The XRD data obtained for the compound with x=0.11 have testified a small amount (~10%) of the orthorhombic phase presented along with the dominant polar rhombohedral phase (Fig. 1). The orthorhombic phase has been successfully refined using space group *Pbam* with $\sqrt{2}a_p*2\sqrt{2}a_p*2a_p$ metric (where a_p is the fundamental perovskite lattice parameter) denoting anti-polar alignment of dipole moments. Further chemical doping with Sm ions leads to an increase in the fraction of the anti-polar orthorhombic phase and the compound with $x = 0.15$ has been considered as single-phase compound with anti-polar orthorhombic structure (Fig. 2). The solid solutions with the dopant concentrations $x > 0.18$ have been characterized by non-polar orthorhombic crystal

structure described by space group *Pbnm* ($\sqrt{2}a_p*\sqrt{2}a_p*2a_p$ metric) which is specific for orthoferrites. Narrow concentration ranges for the two-phase coexistence regions ($\Delta x \sim 0.04$ for R+O_2 phases and $\Delta x \sim 0.03$ for O_2+O_1) imply a high chemical homogeneity of the compounds. Temperature evolution of the crystal structure of the compounds having the two-phase structural state at room temperature testifies intrinsic character of the denoted phase segregation as described below. Extremely narrow (about 1%) concentration range for the single phase state with the anti-polar orthorhombic structure stable at room temperature strongly confirms the mentioned statement.

One can consider the anti-polar orthorhombic phase to be the intermediate phase across the concentration driven transition from the polar rhombohedral phase to the non-polar orthorhombic phase observed in the solid solutions $Bi_{1-x}RE_xFeO_3$ (RE – rare-earth ions La - Sm). It should be noted that the structural data available for the compounds $Bi_{1-x}RE_xFeO_3$ doped with the rare-earth elements having the smaller ionic radii suggest the absence of the anti-polar orthorhombic phase at room temperature [18, 26]. The latter fact is explained by the close values of the ground state energies estimated for the anti-polar and non-polar orthorhombic phases [16, 40]. It is suggested that the crystal structure of the compounds $Bi_{1-x}RE_xFeO_3$ subjected to high temperature transforms directly to the non-polar orthorhombic phase regardless the rare-earth dopant, the transition being accompanied by a drastic (1-2%) decrease in the unit cell volume [12, 20, 41].

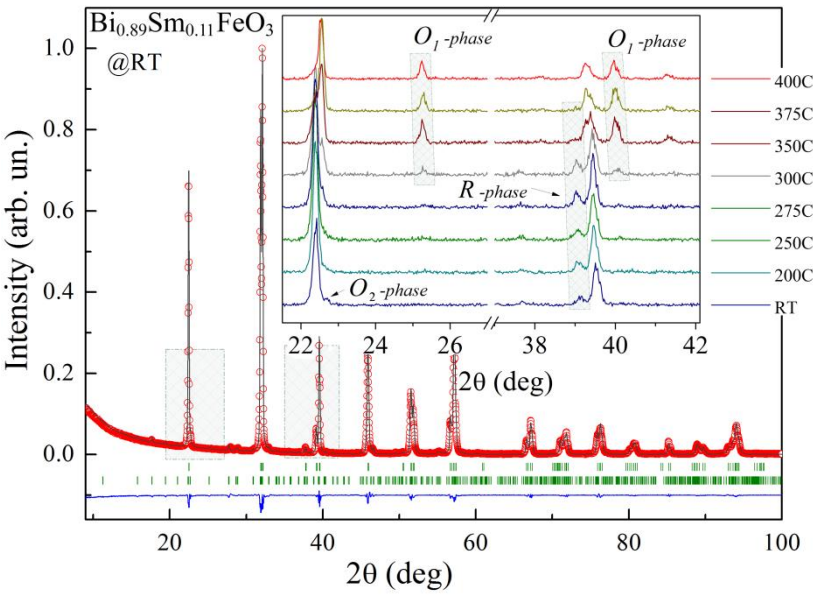

Fig. 1. The XRD pattern of $Bi_{0.89}Sm_{0.11}FeO_3$ recorded at room temperature. Bragg positions attributed to the rhombohedral (upper row) and the orthorhombic phases are marked by vertical ticks. The inset shows evolution of the structural peaks attributed to *R*, O_2- and O_1- structural phases for compound x=0.11 at different temperatures.

Close inspection of the XRD patterns recorded for the phase transition region at elevated temperatures reveals the uncommon features attributed to specific rare-earth elements. The presence of the anti-polar orthorhombic phase over the broad temperature range has been observed for the praseodymium-doped compounds having two-phase structure at room temperature [42]. Such structural stability can be explained in terms of a high hybridization of the chemical bonds formed by praseodymium ions which changes the ground state energies of the related phases [42, 43]. Analysis of the temperature evolution of the crystal structure of the $Bi_{1-x}Sm_xFeO_3$ ($0.1<x<0.15$) compounds representing the rhombohedral-orthorhombic phase boundary region provide additional information about structural stability of the R- and O_2 phases.

The structural data obtained for the compound with x=0.11 demonstrate a gradual increase in the unit cell parameters of the dominant rhombohedral phase with temperature increasing. The minor anti-polar orthorhombic phase observed at room temperature completely disappears at temperatures above 200°C (Fig.1, inset). In the temperature range 200°C - 275°C the crystal structure of the compound is single phase rhombohedral one (Fig.1, inset), while at temperatures of around 300°C the new diffraction peaks characteristic of the non-polar orthorhombic phase appear. At temperature ~400°C the compound becomes single phase with the non-polar orthorhombic structure, the structural transition into the non-polar orthorhombic phase being accompanied by a large decrease in the unit cell volume (~2%). It should be noted that the temperature evolution of the crystal structure observed for this compound, viz. a stabilization of the rhombohedral phase at elevated temperatures and the modification of the unit cell parameters are similar to those estimated for the certain compounds of the systems $Bi_{1-x}La_xFeO_3$ and $Bi_{1-x}Pr_xFeO_3$ having nearly equal ratio of the phases and similar structural parameters at room temperature. Analysis of the temperature evolution of the crystal structure performed for the compounds x=0.12 and 0.13 have testified a decrease in the temperature of the structural transition into the non-polar orthorhombic state. The structural data obtained for the compound x=0.13 have revealed a coexistence of the rhombohedral and the non-polar orthorhombic phases in the temperature range 250°C -350°C. Above 350°C, the crystal structure of the compound is considered to be single phase with the orthorhombic *Pbnm* structure.

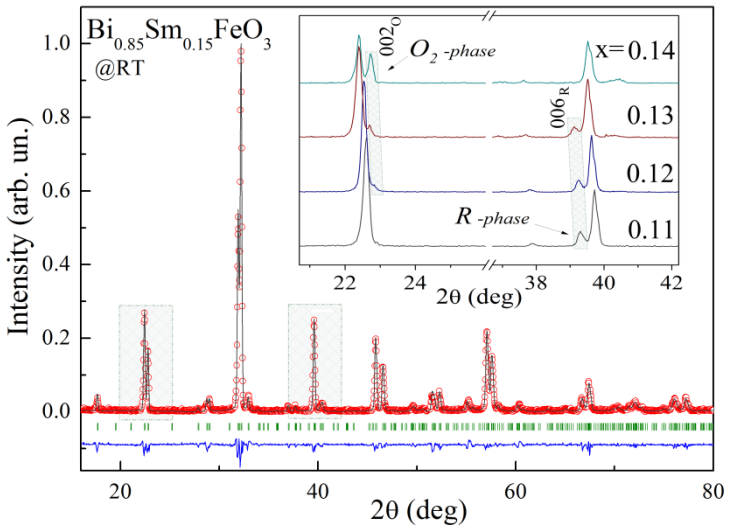

Fig. 2. The XRD pattern of the compound $Bi_{0.85}Sm_{0.15}FeO_3$ recorded at room temperature. Bragg positions denote the single phase orthorhombic phase. The inset shows evolution of the structural peaks attributed to *R*, and O_2- structural phases for compounds x=0.11-0.14 at different temperatures.

It should be noted that the analysis of the structural data performed for the compounds at the morphotropic phase boundary at room temperature did not reveal the formation of any intermediate structural phase across the temperature driven structural transition from the polar rhombohedral phase into the non-polar orthorhombic one. The anti-polar orthorhombic phase observed for the compound with x=0.11 at room temperature disappears at moderate temperatures confirming its metastable character under external stimuli.

In order to specify the temperature evolution of the structural state of the compounds at the morphotropic phase boundary, the HR-TEM measurements have been performed for the x=0.11 sample in the temperature range from 20 to 600°C. The HRTEM investigations have been carried out for a single crystalline composing of the rhombohedral and the orthorhombic phases at room temperature (Fig. 3).

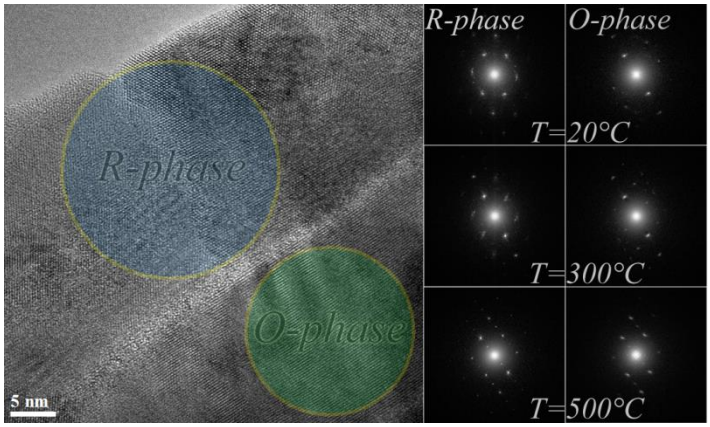

Fig. 3. HRTEM image of the compound with x=0.11 at room temperature denoting a coexistence of both the rhombohedral and orthorhombic phases; the figures on the right side show FFT images calculated for both structural phases in the temperature range 20 - 500°C.

The FFT (Fast Fourier Transforms) pictures calculated for different regions of the HR-TEM image have allowed to estimate a modification of both structural phases occurred upon the temperature increase. The FFT pattern obtained for the upper part of the HRTEM image can be ascribed to the rhombohedral phase (*R3c* space group) and (001) zone axis orientation. The FFT pattern specific to the rhombohedral phase remains stable up to temperatures ~450°C. At the higher temperatures, the FFT pattern of this area is attributed to the non-polar orthorhombic phase described by space group *Pbnm* with (010) zone axis orientation. Analysis of the FFT patterns obtained for other parts of the HR-TEM image can be attributed to the orthorhombic phase. Based on the structural data obtained by XRD method one can assume the presence of the anti-polar orthorhombic phase even though we could not detect spots specific for the anti-polar displacement of the Bi(Sm) ions due to a particular position of the crystalline. The FFT pattern attributed to the orthorhombic phase has not been significantly changed in the measured temperature range (Fig. 3), while some spots become more pronounced, probably due to reduced overlapping of the crystalline layers having different orientations. The results of the HR-TEM measurements have confirmed the structural stability of the rhombohedral phase in the wide temperature range.

Piezoelectric properties

Analysis of the phase transitions based on the XRD data has allowed to estimate the regions of the structural stability of the phases depending on chemical composition and temperature. The results of XRD and TEM measurements did not reveal the presence of any intermediate phase across the temperature-driven phase transitions. The piezoresponse measurements performed for the compounds at the rhombohedral-orthorhombic phase boundary have allowed to examine the piezoresponse as a function of the dopant concentration as well as to estimate structural stability of the phases under electric field.

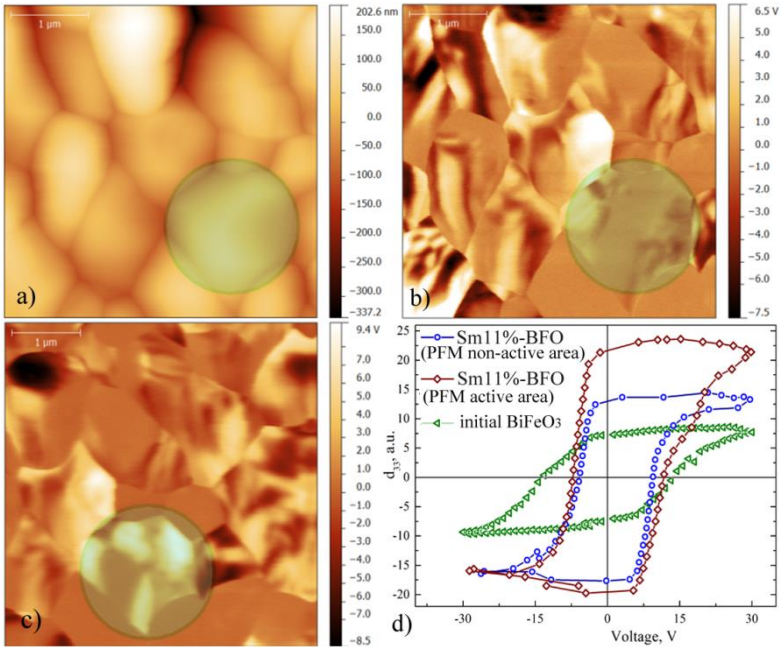

Fig. 4. a) – AFM topography image obtained for the compound x=0.11 in contact mode; b) PFM image (out-of-plane component); c) piezoresponse image after PFM loops measurements made in several spots at one grain (highlighted by circle); d) PFM loops obtained for the compound x=0.11 in different areas and PFM loop measured for the parent compound $BiFeO_3$.

The PFM measurements of the mechanically polished samples with the dopant concentrations x=0.11 - 0.14 have been performed at room temperature. Analysis of the topography testifies the formation of dense ceramics with grains size of about 1 μm (Fig. 4, a). The PFM measurements have allowed to visualize the ferroelectric domain structure and to characterize the particular grains by analyzing the registered piezoresponse and taking into account the XRD data. The presented study is mainly focused on the x=0.11, which is characterized by the coexistence of the dominant polar-active rhombohedral phase and a minor amount of the anti-polar orthorhombic phase, and testifies an ambiguous character of the PFM data. The PFM measurements performed for the compounds with x > 0.11 show a drastic decrease in the piezoresponse signal and confirm the XRD data suggesting the non-polar character of the orthorhombic phases. Taking into account the PFM data, one can confirm that the x=0.11 sample is mainly composed of the polar rhombohedral phase, which is in accordance with the XRD measurements.

The PFM image (Fig. 4, b) shows that the majority of the grains contain several ferroelectric domains with different size and shape. Some of the grains show neutral contrast for both lateral and vertical piezoresponse components. Since piezoresponse hysteresis loops have been obtained for different grains of the doped and parent $BiFeO_3$ compounds, the effect of grain orientation is negligible. The piezoelectric loops have been measured using the same experimental parameters (cantilever stiffness, driving voltage, instrumental parameters of a lock-in amplifier), the presented results have been averaged, so the PFM responses recorded at different areas of the sample can be directly compared, even though the signal is represented using arbitrary units. Piezoresponse hysteresis loops obtained under the application of 30 V attest a switchable character of the electric polarization (Fig. 4, d). In order to estimate phase stability of the doped compound we have measured PFM hysteresis loops at the grains having initially different piezoelectric contrast. The piezoresponse obtained for the doped compound is strongly dependent on the measured area. In the area, having a distinct domain structure, the amplitude of the piezoelectric loops is nearly three times higher than that observed for the parent $BiFeO_3$. It should be noted that the XRD data testify a decrease in the rhombohedral distortion and,

accordingly, in the off-center displacement of the Bi(Sm) ions with increasing x, thus one could expect the opposite behavior of the piezoresponse. Similar evolution of the piezoelectric signal has been observed for the La-doped $BiFeO_3$ compounds with compositions near the rhombohedral-orthorhombic phase boundary [22]. The drastic increase in the PFM signal observed for the compounds of both mentioned systems is most probably caused by significant extrinsic component of the peizoelectric response assosiated with high mobility of the domain walls due to a number of structural defects (e.g. vacancies, local fluctuations of the chemical composition etc.).

The results of the PFM measurements done in the neutral areas (Fig. 4), as attested by both in-plane and out-of-plane components of the piezoresponse, point at the transformation of the anti-polar orthorhombic structure under external electric field. The PFM loops measured in neutral areas testify significantly lower piezoresponse as compared to that measured for the areas showing distinct domain structure, while the amplitude of the piezoresponse is still notably larger than that estimated for the parent compound $BiFeO_3$ (Fig. 4, d). The areas with initially neutral contrast have been modified by external electric field and the regions with distinct piezoresponse have been induced (Fig. 4, b, c). The evolution of the piezoresponse observed for the compound before and after PFM loops measurements can be ascribed to partial transition of the anti-polar orthorhombic phase into the polar active rhombohedral one under applied electric field. It should be noted that no backward transition has been observed during several days after the PFM measurements. The model of the structural transition from the anti-polar orthorhombic phase to the polar rhombohedral phase induced by external electric field has been theoretically predicted in [40] and is considered for $BiFeO_3$-based films and similar ceramics assuming the experimental data [16, 28]. One can also ascribe the appearance of the polar active area to the polarization of the clusters of the rhombohedral phase having nanoscale size and randomly distributed among the anti-polar orthorhombic phase, although this scenario is less probable, assuming the observed images of distinct piezoelectric contrast stable without external electric field.

Conclusions

The crystal structure and piezoelectric properties of the $Bi_{1-x}Sm_xFeO_3$ ceramics have been investigated across the concentration- and temperature-driven transition from the rhombohedral into the orthorhombic phase. The XRD and TEM data obtained for the compounds at the morphotropic phase boundary attest the temperature-driven transition into the non-polar orthorhombic phase occurring without any intermediate phase. The obtained results have confirmed the higher temperature stability of the rhombohedral phase as compared to the anti-polar orthorhombic phase. The PFM measurements have revealed an increased piezoresponse for the compounds having dominant rhombohedral phase as compared to the parent $BiFeO_3$. The enhanced electromechanical properties observed for the compounds at the morphotropic phase boundary are most probably associated with significant extrinsic component of the peizoresponse due to the increased mobility of the domain walls which is specific to the compounds with metastable structural state. The dramatic increase in the piezoelectric signal registered for the grains having no piezoresponse in the initial state can be associated with the electric filed-driven transition of the anti-polar orthorhombic phase into the polar rhombohedral phase.

Acknowledgment

This project work has received funding from the European Union's Horizon 2020 research and innovation programme under the Marie Skłodowska-Curie grant agreement No 778070 – TransFerr – H2020-MSCA-RISE-2017. The authors are also grateful to FCT (projects IF/00819/2014/CP1223/CT0011 and UID/FIS/04564/2016), RFFI (#17-58-45026) and MK-1720.2017.8. Dr. F. Girgsdies and Dr. X. Huang are acknowledged for the X-ray diffraction and TEM measurements, respectively.

References

[1] M. Fiebig, J. Phys. D: Appl. Phys., 38 (2005) R123.
[2] C.-H. Yang, D. Kan, I. Takeuchi, V. Nagarajan, J. Seidel, Phys. Chem. Chem. Phys., 14 (2012) 15953-15962.
[3] S.V. Trukhanov, A.V. Trukhanov, V.G. Kostishin, L.V. Panina, I.S. Kazakevich, V.A. Turchenko, V.V. Kochervinskii, JETP Lett., 103 (2016) 100-105.
[4] V.A. Turchenko, A.V. Trukhanov, I.A. Bobrikov, S.V. Trukhanov, A.M. Balagurov, J. Surf. Invest., 9 (2015) 17-23.
[5] A. Trukhanov, P. Larisa, T. Sergei, T. Vitalii, S. Mohamed, Chin. Phys. B, 25 (2016) 016102.
[6] B. Noheda, and D. E. Cox, Phase Transitions, 79 (2006) 5-20.
[7] V.A. Turchenko, A.V. Trukhanov, I.A. Bobrikov, S.V. Trukhanov, A.M. Balagurov, Crystallogr. Rep., 60 (2015) 629-635.
[8] D. Damjanovic, Appl. Phys. Lett., 97 (2010) 062906-062908.
[9] M. Ahart, M. Somayazulu, R. E. Cohen, P. Ganesh, P. Dera, H.-K. Mao, R. J. Hemley, Y. Ren, P. Liermann, Z. Wu, Nature, 451 (2008) 545-548.
[10] I. O. Troyanchuk, D. V. Karpinsky, M. V. Bushinsky, M. I. Kovetskaya, E. A. Efimova, V. V. Eremenko, J. Exp. Theor. Phys., 113 (2012) 1025-1031.
[11] G. L. Yuan, S. W. Or, J. M. Liu, Z.G. Liu, Appl. Phys. Lett., 89 (2006) 052905-052907.
[12] D. A. Rusakov, A. M. Abakumov, K. Yamaura, A. A. Belik, G. Van Tendeloo, E. Takayama-Muromachi, Chem. Mater., 23 (2010) 285.
[13] D. Kan, C.-J. Cheng, V. Nagarajan, I. Takeuchi, J. Appl. Phys., 110 (2011) 014106.
[14] J.-H. Lee, M.-Ae Oak, H. J. Choi, J. Y. Son, H. M. Jang, J. Mater. Chem., 22 (2012) 1667-1672.
[15] D.V. Karpinsky, I.O. Troyanchuk, A.L. Zheludkevich, O.V. Ignatenko, M.V. Silibin, V.V. Sikolenko, Physics of the Solid State, 58 (2016) 1590-1595.
[16] D. Kan, L. Palova, V. Anbusathaiah, C. J. Cheng, S. Fujino, V. Nagarajan, K. M. Rabe, I. Takeuchi, Adv. Funct. Mater., 20 (2010) 1108-1115.
[17] I. Levin, M. G. Tucker, H. Wu, V. Provenzano, C. L. Dennis, S. Karimi, T. Comyn, T. Stevenson, R. I. Smith, I. M. Reaney, Chem. Mater., 23 (2011) 2166-2175.
[18] I. O. Troyanchuk, D. V. Karpinsky, M. V. Bushinsky, O. S. Mantytskaya, N. V. Tereshko, V. N. Shut, J. Am. Ceram. Soc., 94 (2011) 4502-4506.
[19] D. V. Karpinsky, I. O. Troyanchuk, M. Tovar, V. Sikolenko, V. Efimov, A. L. Kholkin, J. Alloys Compd., 555 (2013) 101-107.
[20] D. V. Karpinsky, I. O. Troyanchuk, M. Tovar, V. Sikolenko, V. Efimov, E. Efimova, V. Ya. Shur, A. L. Kholkin, J. Am. Ceram. Soc., 97 (2014) 2631-2638.
[21] D.V. Karpinsky, I.O. Troyanchuk, V. Sikolenko, V. Efimov, E. Efimova, M. Willinger, A.N. Salak, A.L. Kholkin, J. Mater. Sci., 49 (2014) 6937-6943.
[22] I. O. Troyanchuk, D. V. Karpinsky, M. V. Bushinsky, V. A. Khomchenko, G. N. Kakazei, J. P. Araujo, M. Tovar, V. Sikolenko, V. Efimov, A. L. Kholkin, Phys. Rev. B, 83 (2011) 054109 - 054115.
[23] D. V. Karpinsky, I. O. Troyanchuk, O. S. Mantytskaja, G. M. Chobot, V. V. Sikolenko, V. Efimov, M. Tovar, Phys. Solid State, 56 (2014) 701-706.
[24] A. Perejon, P. E. Sanchez-Jimenez, L. A. Perez-Maqueda, J. M. Criado, J. Romero de Paz, R. Saez-Puche, N. Maso, A. R. West, J. Mater. Chem. C, 2 (2014) 8398-8411.
[25] B. Xu, D. Wang, J. Íñiguez, L. Bellaiche, Adv. Funct. Mater., 23 (2014) 552-558.
[26] D. Arnold, IEEE Trans. Ultrason. Ferroelectr. Freq. Control, 62 (2015) 62-82.

[27] E. Gil-González, A. Perejón, P.E. Sánchez-Jiménez, M.A. Hayward, J.M. Criado, M.J. Sayagués, L.A. Pérez-Maqueda, J. Alloys Compd., 711 (2017) 541-551.
[28] J. Walker, H. Simons, D.O. Alikin, A.P. Turygin, V.Y. Shur, A.L. Kholkin, H. Ursic, A. Bencan, B. Malic, V. Nagarajan, T. Rojac, Sci. Rep., 6 (2016) 19630.
[29] S. Boyn, A.M. Douglas, C. Blouzon, P. Turner, A. Barthélémy, M. Bibes, S. Fusil, J.M. Gregg, V. Garcia, Applied Physics Letters, 109 (2016) 232902.
[30] E. Jartych, T. Pikula, K. Kowal, J. Dzik, P. Guzdek, D. Czekaj, Nanoscale Research Letters, 11 (2016) 234.
[31] W. Yaojin, G. David, B. David, G. Junqi, L. Menghui, L. Jiefang, V. Dwight, Advanced Materials, 23 (2011) 4111-4114.
[32] C. Jia, J. Berakdar, Applied Physics Letters, 95 (2009) 012105.
[33] I. O. Troyanchuk, N. V. Tereshko, D. V. Karpinsky, A. L. Kholkin, M. Kopcewicz, K. Barner, J. Appl. Phys., 109 (2011) 114102.
[34] F. Li, S. Zhang, Z. Xu, X. Wei, J. Luo, T.R. Shrout, Journal of Applied Physics, 108 (2010) 034106.
[35] S. Keisuke, H. Hajime, I. Yuichi, A. Masaki, Advanced Materials, 28 (2016) 8639-8644.
[36] J. Rodríguez-Carvajal, Physica B:, 192 (1993) 55-69.
[37] N. Balke, I. K. Bdikin, S. V. Kalinin, A.L. Kholkin, J. Amer. Ceram. Soc., 92 (2009) 1629–1647.
[38] M. Nomoto, T. Inoshita, Y. Inoue, Y. Horibe, Y. Koyama, MRS Advances, 1 (2016) 573-578.
[39] V.A. Khomchenko, J.A. Paixão, V.V. Shvartsman, P. Borisov, W. Kleemann, D.V. Karpinsky, A.L. Kholkin, Scripta Materialia, 62 (2010) 238-241.
[40] O. E. González-Vázquez, J. C. Wojdeł, O. Diéguez, J. Íñiguez, Phys. Rev. B, 85 (2012) 064119-064128.
[41] S.M. Selbach, T. Tybell, M.-A. Einarsrud, T. Grande, J. Solid State Chem., 183 (2010) 1205-1208.
[42] D.V. Karpinsky, I.O. Troyanchuk, M. Willinger, V.A. Khomchenko, A.N. Salak, V. Sikolenko, M.V. Silibin, J. Mater. Sci., 52 (2017) 9355-9362.
[43] D.V. Karpinsky, E.A. Eliseev, F. Xue, M.V. Silibin, A. Franz, M.D. Glinchuk, I.O. Troyanchuk, S.A. Gavrilov, V. Gopalan, L.-Q. Chen, A.N. Morozovska, npj Comput. Mater., 3 (2017) 20.